Journal homepage http://revistas.unitru.edu.pe/index.php/SSMM

SELECCIONES MATEMÁTICAS
Universidad Nacional de Trujillo
ISSN: 2411-1783 (Online)
2021; Vol. 8(2): 228-234.

Rotational gravity-capillary waves generated by a moving disturbance

Ondas rotacionales de gravedad-capilaridad generadas por el paso de una perturbación

Marcelo Flamarion

Received, Jul. 06, 2021 *Accepted, Aug. 10, 2021*

How to cite this article:
Flamarion, M. *Rotational gravity-capillary waves generated by a moving disturbance*. Selecciones Matemáticas. 2021;8(2):228–234. http://dx.doi.org/10.17268/sel.mat.2021.02.02

Abstract

Nonlinear gravity-capillary waves generated by the passage of a pressure distribution over a sheared channel with constant vorticity are investigated. The problem is modeled using the full Euler equations. The harmonic part of the velocity field is formulated in a canonical domain through the use of the conformal mapping, which flattens the fluid domain onto a strip. The Froude number is considered to be nearly-critical and the Bond number critical. The shear effect changes drastically the pattern of the generated waves for large times. Moreover, depending on the intensity of the vorticity, the wave solutions can become smoother with small amplitudes.

Keywords . Water waves, gravity-capillary waves, Euler equations, conformal mappings.

Resumen

Se estudian ondas no lineales de gravedad-capilaridad generadas por el paso de una distribución de presión sobre un canal cizallado con vorticidad constante. El problema es modelado usando las ecuaciones de Euler. La parte harmónica del campo de velocidades es formulada en un dominio canónico a través de la representación conforme, que aplana el dominio del fluido en una franja. El número de Froude es considerado casi crítico y el número de Bond crítico. El efecto de la vorticidad cambia radicalmente el patrón de las ondas generadas para tiempos largos. Adicionalmente, dependiendo da la intensidad de la vorticidad, las soluciones pueden tornarse más suaves y con pequeñas amplitudes.

Palabras clave. Ondas acuáticas, ondas de gravedad-capilaridad, ecuaciones de Euler, representación conforme.

1. Introduction. Generated waves due to a disturbance moving over a water surface have several physical applications. For example, ship wakes [2], waves generated due to the formation of storms in high seas [3] and experiments in laboratory are conducted daily using external forces as a mechanism to generate waves [15].

In the absence of surface tension, the fundamental parameters for describing the pattern of the generated waves are the amplitude of the applied pressure over the free surface and the Froude number, namely,

$$F = \frac{U_0}{\sqrt{gh_0}}.$$

Here, U_0 is the constant speed of the moving disturbance, g is the force of gravity and h_0 is the depth of the channel. This problem has been extensively studied in the forced Korteweg-de Vries (fKdV) framework as well as in the Euler equations. Therefore, it is hard to give a comprehensive overview of contributions. For the interested reader, we mention [1, 17, 14, 11, 7, 8].

*UFRPE/Rural Federal University of Pernambuco, UACSA/Unidade Acadêmica do Cabo de Santo Agostinho, BR 101 Sul, 5225, 54503-900, Ponte dos Carvalhos, Cabo de Santo Agostinho, Pernambuco, Brazil. (marcelo.flamarion@ufrpe.br).

When the effects of surface tension are no longer neglected, another parameter becomes important in the study of the pattern of the generated waves, namely, the Bond number

$$B = \frac{\sigma}{\rho g h_0^2},$$

where σ is the coefficient of the surface tension and ρ is the constant density of the fluid [13]. The classical Korteweg-de Vries equation (KdV) can still be used as a model to study gravity-capillary waves in the weakly nonlinear, weakly dispersive regime with an external force with small amplitude. However, a higher-order model is required to study the problem when the Bond number is nearly-critical ($B \approx 1/3$) since its dispersive term vanishes approaching asymptotically to the inviscid Burgers equation and solitary waves are no longer appropriate [5]. Assuming $F \approx 1$ and $B \approx 1/3$, Milewski and Vanden-Broeck [13] derived a fifth-order fKdV considering an obstacle with small amplitude. They classified the flow over the obstacles identifying its main features and computed unsteady solitary wave solutions with small oscillating tails. Interactions of generated waves above two obstacles were later investigated in [9].

Although there have been many studies on gravity-capillary waves in the weakly nonlinear and weakly dispersive regime, numerical solutions of the full Euler equations have been little explored, especially under a background shear flow. In the absence of a pressure distribution, Fracius et al. [10] studied gravity-capillary waves propagating steadily in finite depth channel with a linear shear current. They computed traveling waves analytically using a classical Stokes procedure and compared their solutions with numerical ones. Hanazaki et al. [12] solved the Euler equations in the presence of a topography with a uniform flow using the body-fitted curvilinear coordinates and compared the results with both the third-order fKdV and the fifth-order fKdV in the resonant regime $F = 1$ and intermediate capillary effects ($B \approx 1/3$). Short wave radiation was observed when the effects of surface tension are weak ($B < 1/3$). Moreover, the train of solitary waves propagating upstream radiates short linear waves whose phase speed is equal to the upstream-advancing speed of the solitary waves. The wave train going upstream is captured by the fifth-order fKdV equation, however it predicts waves of longer length, as expected since the fKdV model agrees well with the full nonlinear model only in the long wave regime.

In this work, we investigate numerically the behaviour of gravity-capillary waves excited by a moving pressure in the presence of a background shear flow under the nearly-resonant conditions $F \approx 1$ and $B = 1/3$. To the best of our knowledge there are no articles about excited gravity-capillary waves over a shear flow. The vorticity changes the pattern of the generated waves as if the critical Froude number was shifted by it. Depending on the intensity of the vorticity the generated waves may become smoother with smaller amplitudes.

This article is organized as follows. In section 1 we present the mathematical formulation of the Euler equations. In section 2 we use the conformal mapping technique to rewrite the Euler equations in the canonical domain, which is a uniform strip, and present a numerical method to solve them. In section 3 we present the numerical results and the conclusion in section 4.

2. Mathematical Formulation. We consider a two-dimensional incompressible flow of an inviscid fluid with constant density (ρ) in a finite depth channel (h_0) with constant vorticity (Ω_0) and in the presence of the gravity force (g) and surface tension (σ). Besides, a moving pressure distribution (P) with constant speed (U_0) is applied over the free surface ($\tilde{\zeta}(x,t)$). Under these conditions the velocity field in the bulk fluid can be written as

$$\nabla\tilde{\phi}(x,y,t) + (-\Omega_0 y, 0),$$

where $\tilde{\phi}(x,y,t)$ is the harmonic component of the velocity field. The governing equations that model the problem are

$$\begin{aligned}
&\Delta\tilde{\phi} = 0 \ \text{ for } \ -h_0 < y < \tilde{\zeta}(x,t),\\
&\tilde{\phi}_y = 0 \ \text{ at } \ y = -h_0,\\
&\tilde{\zeta}_t - \Omega_0\tilde{\zeta}\tilde{\zeta}_x + \tilde{\phi}_x\tilde{\zeta}_x - \tilde{\phi}_y = 0 \ \text{ at } \ y = \tilde{\zeta}(x,t),\\
&\tilde{\phi}_t + \frac{1}{2}(\tilde{\phi}_x^2 + \tilde{\phi}_y^2) - \Omega_0\tilde{\zeta}\tilde{\phi}_x + g\tilde{\zeta} + \Omega_0\tilde{\psi} - \sigma\frac{\tilde{\zeta}_{xx}}{(1+\tilde{\zeta}_x^2)^{3/2}} = -\frac{P(x+U_0t)}{\rho} \ \text{ at } \ y = \tilde{\zeta}(x,t),
\end{aligned} \tag{2.1}$$

where $\tilde{\psi}$ is the harmonic conjugate of $\tilde{\phi}$. Using the typical wavelength h_0 as the horizontal and vertical length, $(gh_0)^{1/2}$ as the velocity potential scale, $(h_0/g)^{1/2}$ as the time scale, and $\rho g h_0$ as the pressure scale

as done in [7], we obtain the following dimensionless equations

$$\begin{aligned}
&\Delta\tilde{\phi} = 0 \ \text{ for } \ -1 < y < \tilde{\zeta}(x,t),\\
&\tilde{\phi}_y = 0 \ \text{ at } \ y = -1,\\
&\tilde{\zeta}_t - \Omega\tilde{\zeta}\tilde{\zeta}_x + \tilde{\phi}_x\tilde{\zeta}_x - \tilde{\phi}_y = 0 \ \text{ at } \ y = \tilde{\zeta}(x,t),\\
&\tilde{\phi}_t + \frac{1}{2}(\tilde{\phi}_x^2 + \tilde{\phi}_y^2) - \Omega\tilde{\zeta}\tilde{\phi}_x + \tilde{\zeta} + \Omega\tilde{\psi} - B\frac{\tilde{\zeta}_{xx}}{(1+\tilde{\zeta}_x^2)^{3/2}} = -P(x+Ft) \ \text{ at } \ y = \tilde{\zeta}(x,t),
\end{aligned} \tag{2.2}$$

where $F = U_0/(gh_0)^{1/2}$ is the Froude number, $B = \sigma/(\rho g h_0^2)$ is the Bond number and $\Omega = \Omega_0 h_0/(gh_0)^{1/2}$ is the dimensionless vorticity. For computational purposes, it is convenient to rewrite the equations (2.2) in the moving framework $x \to x + Ft$. For this reason, we define

$$\tilde{\zeta}(x - Ft, t) = \bar{\zeta}(x,t), \ \ \tilde{\phi}(x - Ft, y, t) = \bar{\phi}(x,y,t). \tag{2.3}$$

Substituting (2.3) in (2.2) yields the dimensionless system

$$\begin{aligned}
&\Delta\bar{\phi} = 0 \ \text{ for } \ -1 < y < \bar{\zeta}(x,t),\\
&\bar{\phi}_y = 0 \ \text{ at } \ y = -1,\\
&\bar{\zeta}_t + (F - \Omega\bar{\zeta} + \bar{\phi}_x)\bar{\zeta}_x - \bar{\phi}_y = 0 \ \text{ at } \ y = \bar{\zeta}(x,t),\\
&\bar{\phi}_t + \frac{1}{2}(\bar{\phi}_x^2 + \bar{\phi}_y^2) + (F - \Omega\bar{\zeta})\bar{\phi}_x + \bar{\zeta} + \Omega\bar{\psi} - B\frac{\bar{\zeta}_{xx}}{(1+\bar{\zeta}_x^2)^{3/2}} = -P(x) \ \text{ at } \ y = \bar{\zeta}(x,t).
\end{aligned} \tag{2.4}$$

We are interested in understanding the behaviour of generated waves due to the passage of the pressure distribution. In the following, all graphics are be plotted in moving frame.

3. Conformal mapping and numerical methods. We solve numerically the system (2.1) in the same fashion as Dyachenko et al. [4]. Initially, we construct a time-dependent conformal mapping

$$z(\xi,\eta,t) = x(\xi,\eta,t) + iy(\xi,\eta,t),$$

which flattens the free surface and maps a strip of width D onto the fluid domain. The conformal mapping satisfyies the boundary conditions

$$y(\xi,0,t) = \overline{\zeta}(x(\xi,0,t),t) \ \text{ and } \ y(\xi,-D,t) = -1.$$

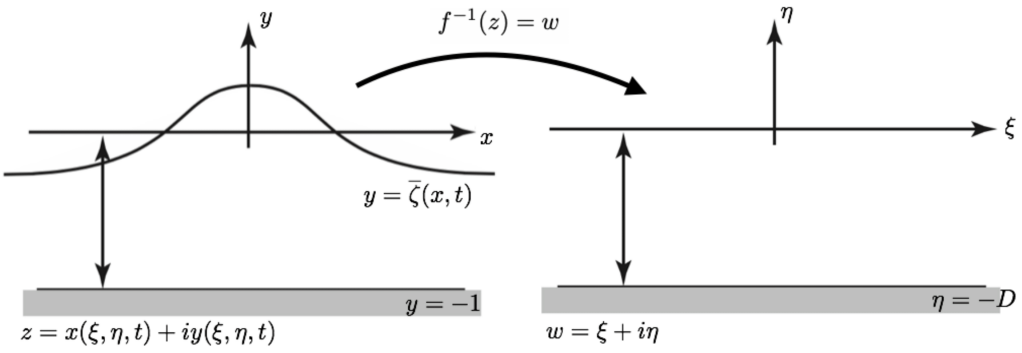

Figure 3.1: The conformal mapping. The free surface is flattened out in the canonical domain.

We recall that one of the the main features of conformal mappings is that they preserve angles, thus the vertical height of the canonical strip has to adjust itself to preserve angles at each time. Consequently, D is a function of time.

Consider $\bar{\psi}(x(\xi,\eta,t), y(\xi,\eta,t), t)$ the harmonic conjugate of $\bar{\phi}(x(\xi,\eta,t), y(\xi,\eta,t), t)$, and

$$\phi(\xi,\eta,t) = \bar{\phi}(x(\xi,\eta,t), y(\xi,\eta,t), t)$$

the potential velocity in the canonical domain with its harmonic conjugate denoted by $\psi(\xi,\eta,t)$. Let $\mathbf{\Phi}(\xi,t)$ and $\mathbf{\Psi}(\xi,t)$ be their traces along $\eta = 0$ and by $\mathbf{X}(\xi,t)$, $\mathbf{Y}(\xi,t)$ denote the horizontal and vertical free

surface coordinates at $\eta = 0$. Substituting these variables in Kinematic and Bernoulli conditions $(2.4)_{3,4}$ we obtain

$$\mathbf{Y}_t = \mathbf{Y}_\xi \mathcal{C}\left[\frac{\mathbf{\Theta}_\xi}{J}\right] - \mathbf{X}_\xi \frac{\mathbf{\Theta}_\xi}{J}, \tag{3.1}$$

$$\mathbf{\Phi}_t = -\mathbf{Y} - \frac{1}{2J}(\mathbf{\Phi}_\xi^2 - \mathbf{\Psi}_\xi^2) + \mathbf{\Phi}_\xi \mathcal{C}\left[\frac{\mathbf{\Theta}_\xi}{J}\right] - \frac{1}{J}(F - \Omega\mathbf{Y})\mathbf{X}_\xi \mathbf{\Phi}_\xi + \Omega\mathbf{\Psi} + B\frac{\mathbf{X}_\xi \mathbf{Y}_{\xi\xi} - \mathbf{Y}_\xi \mathbf{X}_{\xi\xi}}{J^{3/2}} - P(\mathbf{X}),$$

where $\mathbf{\Theta}_\xi(\xi, t) = \mathbf{\Psi}_\xi + F\mathbf{Y}_\xi + \Omega\mathbf{Y}\mathbf{Y}_\xi$, $\mathcal{C}$ is the operator

$$\mathcal{C} = \mathcal{F}^{-1}_{k\neq 0} i \coth(k_j D)\mathcal{F}_{k\neq 0},$$

$J = \mathbf{X}_\xi^2 + \mathbf{Y}_\xi^2$ is the Jacobian of the conformal mapping evaluated at $\eta = 0$ and

$$\begin{aligned} \mathbf{X}_\xi &= 1 - \mathcal{C}\big[\mathbf{Y}_\xi\big], \\ \mathbf{\Phi}_\xi &= -\mathcal{C}\big[\mathbf{\Psi}_\xi\big]. \end{aligned} \tag{3.2}$$

Fourier modes are given by

$$\mathcal{F}_{k_j}[g(\xi)] = \hat{g}(k_j) = \frac{1}{2L}\int_{-L}^{L} g(\xi) e^{-ik_j\xi}\, d\xi,$$

$$\mathcal{F}^{-1}_{k_j}[\hat{g}(k_j)](\xi) = g(\xi) = \sum_{j=-\infty}^{\infty} \hat{g}(k_j) e^{ik_j\xi},$$

where $k_j = (\pi/L)j$, $j \in \mathbb{Z}$. We choose D so that the canonical domain and physical domain have the same length. Therefore,

$$D = 1 + \frac{1}{2L}\int_{-L}^{L} \mathbf{Y}(\xi, t) d\xi.$$

More details of this numerical method can be found in [7, 6].

In the following section we consider the computational domain $[-L, L]$, with a uniform grid with N points and step $\Delta\xi = 2L/N$. All derivatives in ξ are performed using the Fast Fourier Transform (FFT) [16]. In addition, the time advance of the system (3.1) is computed through the Runge-Kutta fourth order method (RK4) with time step Δt. In the following simulations, we use the parameters: $L = 500$, $N = 2^{13}$, and $\Delta t = 0.01$. Moreover, we take the shape profile of the distribution of pressure to be

$$P(x) = \epsilon \exp\Big(-x^2/w\Big),$$

where $w = 10$ and $\epsilon = 0.01$.

4. Numerical results. In this section we consider the Euler equations and investigate the effects of the nonuniform current on the generated waves. We focus on the nearly-critical regime ($F \approx 1$) when the Bond number is critical ($B = 1/3$).

Under these conditions, using a higher-order forced Korteweg-de Vries equation, Milewski and Vanden-Broeck [13] classified the flow over an obstacle into three types. Here, we choose different values of F to obtain these distinct regimes and then turn on the vorticity to analyse its consequences.

Firstly, let us consider the subcritical case. In this regime, the flow is mainly characterised by the formation of an upstream transient and the generation of depression solitary waves that propagate downstream. When the vorticity is turned on, we observe that negative values of it tend to linearise the solution, in the sense that the amplitude of the generated waves become very small and the frequency in which depression solitary waves are generated decreases.

The result dynamic is a depression solitary wave located above the obstacle. In addition, when the vorticity is positive the upstream waves become smoother with small amplitude, but these depression waves are generated at a higher frequency.

A slightly increase of the amplitude of the upstream waves is also observed. Details of this dynamic are displayed in Figure 4.1.

In the resonant regime, there is a periodic generation of depression solitary downstream waves with sharp crests for negative values of the vorticity and a transient propagating upstream. Positive and small

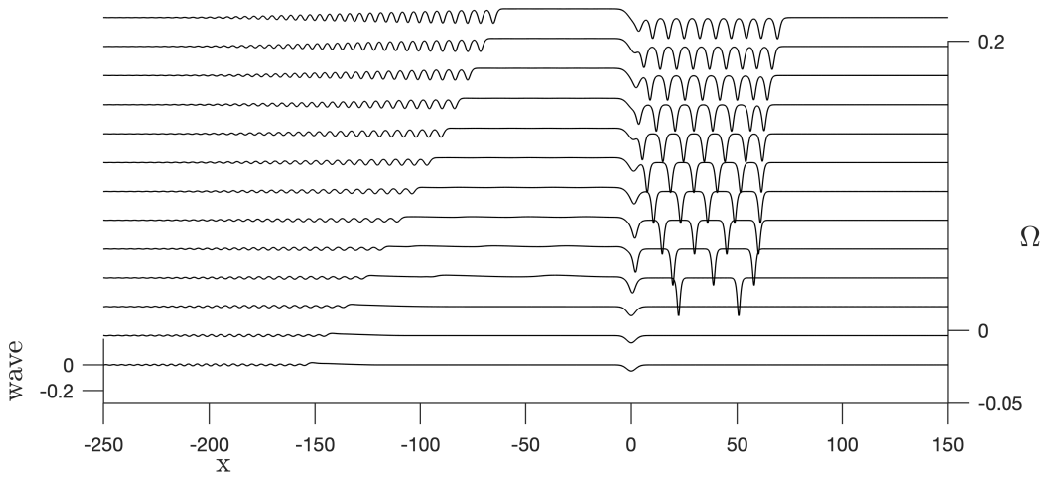

Figure 4.1: Solutions of (2.4) at time $t = 1000$ for different values of Ω with $F = 0.891$.

values of the vorticity leads to the formation of a well defined undular bore structure with an increasing of the amplitudes of the upstream waves and a decreasing in the downstream waves. We point out that the results are qualitatively similar to the ones when the vorticity is neglected. It occurs because the vorticity acts as a perturbation of the Froude number, which in this case is critical. Typical solutions with different values of the vorticity are shown in Figure 4.2. As it can be seen, when the vorticity is positive and larger, the undular bore is narrowed and the downstream waves flattened.

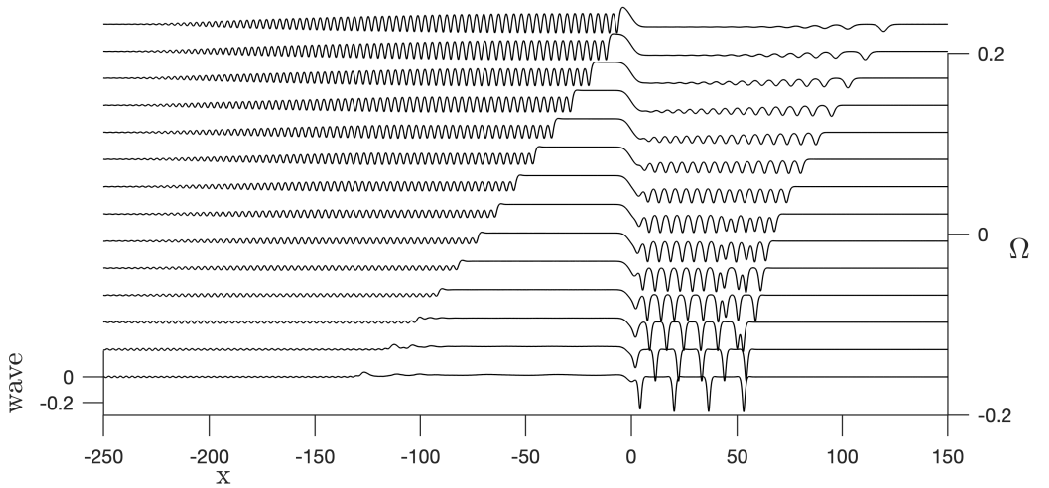

Figure 4.2: Solutions of (2.4) at time $t = 1000$ for different values of Ω with $F = 1$.

Lastly, we consider the supercritical case. The main feature in this regime is the formation of a undular bore headed by a wave train with a train of waves propagating downstream. When the vorticity is added to the problem, we notice that positive values of it tend to linearise the solution similar to what happens to the subcritical case. However, a steady elevation wave takes place over the obstacle followed by depression solitary waves propagating downstream. In addition, negative values of the vorticity parameter leads to a formation of a undular bore above the obstacle led by a wave train propagating upstream as it can be seen in Figure 4.3.

Regarding generated waves, the vorticity plays a very important role in the dynamic of the flows. Although in many problems the vorticity is neglected, here we see that even for small values of the vorticity the flow can change drastically at large times.

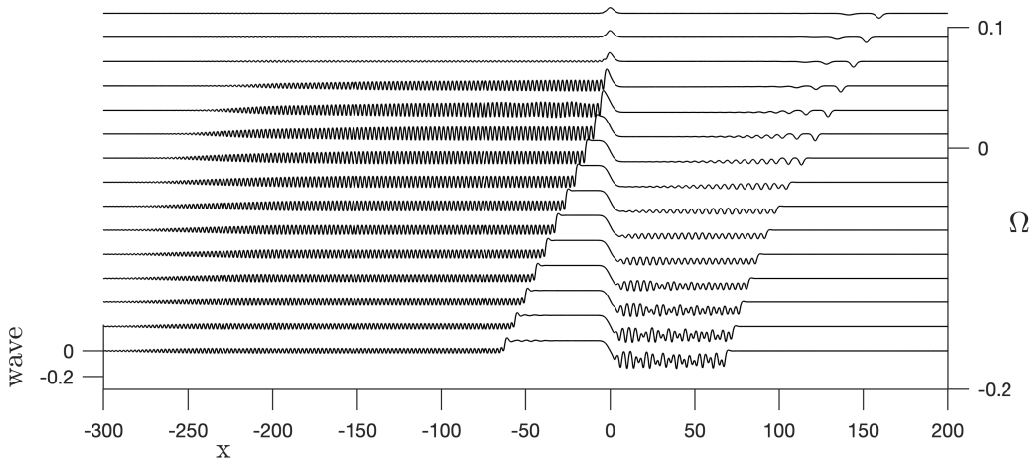

Figure 4.3: Solutions of (2.4) at time $t = 1000$ for different values of Ω with $F = 1.1$.

5. Conclusions. In this paper, we have studied the dynamic of gravity-capillary waves excited by a moving disturbance in a vertically sheared channel using the full Euler equations. Through the conformal mapping technique, we showed that in certain regimes the vorticity tend to smoothen the wave solutions and somewhat linearise them. The sheared current affects not only qualitatively the behaviour of the generated waves, but also quantitatively. Therefore, assuming that the flow is irrotational in certain types of problems can be misleading.

6. Acknowledgements. The author is grateful to IMPA-National Institute of Pure and Applied Mathematics for the research support provided during the Summer Program of 2020 and to Federal University of Paraná for the visit to the Department of Mathematics.

ORCID and License
Marcelo Flamarion https://orcid.org/0000-0001-5637-7454

References

[1] Akylas TR. On the excitation of long nonlinear water waves by a moving pressure distributions. J Fluid Mech. 1984; 141:455-466. DOI: 10.1017/S0022112084000926.
[2] Baines P. Topographic effects in stratified flows. Cambridge: Cambridge University Press; 1995.
[3] Johnson RS. Models for the formation of a critical layer in water wave propagation. Phil Trans R Soc A. 2012; 370:1638-1660. DOI: 10.1098/rsta.2011.0456.
[4] Dyachenko AL, Zakharov VE, Kuznetsov EA. Nonlinear dynamics of the free surface of an ideal fluid. Plasma Phys. 1996; 22:916-928.
[5] Falcon E, Laroche C, Fauve S. Observation of depression solitary surface waves on a thin fluid layer Phys Rev Lett. 2002;89:204501-1-204501-4.
[6] Flamarion MV, Ribeiro-Jr R. An iterative method to compute conformal mappings and their inverses in the context of water waves over topographies Int J Numer Meth Fl. 2021; 93(11):3304-3311. DOI: 10.1002/fld.5030.
[7] Flamarion MV, Milewski PA, Nachbin A. Rotational waves generated by current-topography interaction. Stud Appl Math. 2019; 142: 433-464. DOI: 10.1111/sapm.12253.
[8] Flamarion MV. Rotational flows over obstacles in the forced Korteweg-de Vries framework. Selecciones Matematicas. 2021; 8(1):125-130. DOI: 10.17268/sel.mat.2021.01.12.
[9] Flamarion MV, Ribeiro-Jr R. Gravity-capillary flows over obstacles for the fifth-order forced Korteweg-de Vries equation. J. Eng Math. 2021; 129:17. DOI: 10.1007/s10665-021-10153-z.
[10] Fracius M, Hsu HC. Kharif C, Montalvo P. Gravity-capillary waves in finite depth on flows of constant vorticity. Proc R Soc Lond A. 2016; 472:20160363.
[11] Grimshaw R, Maleewong M. Stability of steady gravity waves generated by a moving localized pressure disturbance in water of finite depth. Phys Fluids. 2013:25:076605. DOI: 10.1063/1.4812285.
[12] Hanazaki H, Hirata M, Okino S. Radiation of short waves from the resonantly excited capillary-gravity waves. J. Fluid Mech. 2010;810: 5-24. DOI: 10.1017/jfm.2016.702
[13] Milewski, PA, Vanden-Broeck JM. Time dependent gravity-capillary flows past an obstacle Wave Motion. 1999; 29:63-79.

[14] Milewski PA. The Forced Korteweg-de Vries equation as a model for waves generated by topography. CUBO A mathematical Journal. 2004; 6:33-51.
[15] Pratt LJ. On nonlinear flow with multiple obstructions. J Atmos Sci. 1984; 41:1214-1225. DOI: 10.1175/1520-0469.
[16] Trefethen LN. Spectral Methods in MATLAB. Philadelphia: SIAM; 2001.
[17] Wu TY. Generation of upstream advancing solitons by moving disturbances. J. Fluid Mech. 1987; 184: 75-99. DOI: 10.1017/S0022112087002817.